Pharmacological Validation of *Trypanosoma brucei* Phosphodiesterases as Novel Drug Targets

Harry P. de Koning,[1] Matthew K. Gould,[1] Geert Jan Sterk,[4] Hermann Tenor,[2] Stefan Kunz,[3] Edith Luginbuehl,[3] and Thomas Seebeck[3]

[1]Institute of Infection, Immunity and Inflammation, College of Medical, Veterinary and Life Sciences, University of Glasgow, United Kingdom; [2]Nycomed GmbH, Konstanz, Germany; [3]Institute of Cell Biology, University of Bern, Switzerland; and [4]Mercachem BV, GE Nijmegen, The Netherlands

The development of drugs for neglected infectious diseases often uses parasite-specific enzymes as targets. We here demonstrate that parasite enzymes with highly conserved human homologs may represent a promising reservoir of new potential drug targets. The cyclic nucleotide-specific phosphodiesterases (PDEs) of *Trypanosoma brucei*, causative agent of the fatal human sleeping sickness, are essential for the parasite. The highly conserved human homologs are well-established drug targets. We here describe what is to our knowledge the first pharmacological validation of trypanosomal PDEs as drug targets. High-throughput screening of a proprietary compound library identified a number of potent hits. One compound, the tetrahydrophthalazinone compound A (Cpd A), was further characterized. It causes a dramatic increase of intracellular cyclic adenosine monophosphate (cAMP). Short-term cell viability is not affected, but cell proliferation is inhibited immediately, and cell death occurs within 3 days. Cpd A prevents cytokinesis, resulting in multinucleated, multiflagellated cells that eventually lyse. These observations pharmacologically validate the highly conserved trypanosomal PDEs as potential drug targets.

Kinetoplastid protozoa (*Kinetoplastida*, *Excavata* [1]) cause severe diseases of humans and/or their domestic animals. In sub-Saharan Africa, the fatal human African trypanosomiasis (HAT, sleeping sickness) is caused by *Trypanosoma brucei* subspecies and threatens 38 countries. The therapeutic armamentarium against sleeping sickness and many other protozoan infections is extremely limited and ineffective, with almost no new drugs introduced for decades [2]. In addition, the standard medication against late-stage sleeping sickness—melarsoprol—is encountering increasing problems with drug refractoriness [3, 4]. Although many compounds with antiparasitic activity have been reported, new paradigms are required for a more efficient development of urgently required antiparasite chemotherapies.

The development of antiparasitic compounds has long focused on parasite-specific targets. This approach has generated some promising lead compounds [5–7] but often encountered difficulties during the transition from basic research to drug development. We here show that a class of enzymes whose catalytic domains are highly conserved between *T. brucei* and its human host, the cyclic nucleotide-specific phosphodiesterases (PDEs), are promising drug targets. Human PDEs are being intensely investigated as drug targets for numerous clinical conditions, and several PDE-inhibitor based drugs are on the market [8]. The genomes of *T. brucei* and all other kinetoplastids were analyzed to date code for 4 distinct PDE families (PDEs A–D; [8]). Their catalytic domains are structurally highly similar to those of the human PDEs ([10]; Hengming Ke, University of North Carolina, personal communication, September 2010). In *T. brucei*, the PDE-B

Received 16 June 2011; accepted 9 September 2011; electronically published 30 January 2012.

Presented in part: Fourth Kinetoplastid Molecular Cell Biology meeting, Woods Hole, Massachusetts 8–12 April 2011. Abstract 2E.

Correspondence: Thomas Seebeck, PhD, Institute of Cell Biology, University of Bern, Baltzerstrasse 4, CH-3012 Bern, Switzerland (thomas.seebeck@izb.unibe.ch).

The Journal of Infectious Diseases 2012;206:229–37

DOI: 10.1093/infdis/jir857

family consists of 2 highly similar enzymes (75.3% overall sequence identity) that are coded for by 2 tandemly arranged genes (located on chromosome 9 in the *T. brucei* genome; [9]). Despite their similarity, TbrPDEB1 and TbrPDEB2 show distinct subcellular localizations [10]. The 2 enzymes TbrPDEB1 and TbrPDEB2 are the predominant controlling elements of intracellular cyclic adenosine monophosphate (cAMP) levels, and their disruption by RNA interference (RNAi) both dramatically increases intracellular cAMP and induces complete trypanosome cell lysis, both in culture and in vivo [11]. The current study identifies a class of potent small-molecule inhibitors of TbrPDEB1 and TbrPDEB2 by high-throughput screening of a chemical library. A representative compound, compound A (Cpd A), causes a rapid and sustained elevation of intracellular cAMP that leads to parasite cell death through inhibition of cytokinesis during cell division. Because PDEs are highly conserved between host and parasite, and because human PDEs are well-explored drug targets, using parasite PDEs as drug targets allows exploitation of the existing vast expertise in developing PDE inhibitors against human PDEs. The study thus demonstrates that parasite enzymes that are highly similar to well-studied human drug targets represent an interesting reservoir of new parasitic drug targets. Using this strategy, we identified PDE inhibitors as a new generation of trypanocidal agents that represent a completely new chemical class and show no cross-resistance with existing drugs.

MATERIALS AND METHODS

Strains and Cultures

The trypanosome line used was strain MiTat1.2(221) [12]. Strain TbAT1KO was constructed by deletion of the TbAT1/P2 transporter from MiTat1.2(221) and consequently was resistant to the veterinary trypanocide diminazene [13, 14]. Strain B48 was derived from TbAT1KO by stepwise adaptation to pentamidine in vitro and has lost the high-affinity pentamidine transporter [15], rendering it highly resistant to both pentamidine and melarsoprol [16]. Strains were grown as bloodstream forms in HMI-9 medium [17]. Ex vivo parasites were purified from whole rat [18], and purified trypanosomes were maintained in HMI-9 medium.

High-Throughput Screening

A proprietary library of >400 000 compounds was screened using a homogenous assay that determines [^{3}H]-cAMP hydrolyzing PDE activity by scintillation proximity assay (SPA). In a first step, PDE activity hydrolyzes [^{3}H]-cAMP into [^{3}H]-5′AMP. In a second step, substrate and product are distinguished by addition of SPA yttrium silicate beads (GE Healthcare). In the presence of zinc sulfate, the linear [^{3}H]-5′AMP binds to the beads, whereas the cyclic [^{3}H]-cAMP does not. Close proximity of bound [^{3}H]-5′AMP then allows radiation from the tritium to the scintillant within the beads, resulting in a measurable signal, whereas the unbound, hence distant [^{3}H]-cAMP does not generate this signal. The enzymatic reaction was conducted in a total assay volume of 100 μL, comprising 20 mmol/L Tris (pH 7.4) supplemented with bovine serum albumin (0.1 mg mL^{-1}) and 5 μmol/L Mg^{2+} in the presence of 0.5 μmol/L cAMP substrate, containing ~50 000 cpm of [^{3}H]-cAMP, and test compound. Recombinant TbrPDEB1 was added in a quantity that resulted in 10%–20% hydrolysis of cAMP. The reaction was initiated by adding the substrate, followed by an incubation for 15 minutes at 37°C. Adding SPA beads with zinc sulphate (50 μL) terminated the reaction, and the SPA signal was analyzed by standard luminescence detection devices. The final concentration of solvent (1% dimethyl sulfoxide [DMSO]) was identical in all assays and did not affect enzymatic activity. In the initial screening campaign, all compounds were added at 10 μmol/L. Compounds showing ≥50% inhibition of TbrPDEB1 activity were retested. The Z factor was 0.716 in the primary screen and 0.740 in the retesting of positive candidates. About 600 compounds showed half-maximal inhibitory concentration (IC_{50}) values for TbrPDEB1 inhibition of ≤5 μmol/L.

Expression of Recombinant TbrPDEB1

TbrPDEB1 was expressed in SF21 insect cells. TbrPDEB1 complementary DNA was amplified by polymerase chain reaction (PCR) and cloned into the pCR-Bac vector (Invitrogen). SF21 cells were infected with a high-titer virus supernatant, and infected cells were cultured for 48–72 hours to allow optimal protein expression. Cells were collected in 20 mmol/L Tris pH 8.2, 140 mmol/L sodium chloride, 3.8 mmol/L potassium chloride, 1 mmol/L ethylene glycol tetraacetic acid, 1 mmol/L magnesium $chloride_2$, 10 mmol/L ß-mercaptoethanol, 2 mmol/L benzamidine, 0.4 mmol/L Pefabloc, 10 μmol/L leupeptin, 10 μmol/L pepstatin A, and 5 mmol/L soybean trypsin inhibitor. After sonication, a 1000 *g* supernatant was used for enzyme assays.

Determination of PDE Activity

PDE activity of Triton X-100 lysates of whole trypanosomes or of recombinant enzyme was determined by published procedures [19, 20]. Enzyme concentrations were always adjusted so that <20% of substrate was consumed. Blank values (measured in the presence of denatured protein) were always <2% of total radioactivity.

Cell Proliferation Assay

Test compounds were serially diluted in 96-well plates in HMI-9 medium [21]. After 48 hours of incubation, 20 μL of 0.5 mmol/L resazurin in phosphate-buffered saline (PBS) was added. Fluorescence was measured after an additional

24 hours with excitation and emission filters of 544 and 590 nm, respectively. The detailed assessments of efficacy against *T. brucei* strains of differing drug sensitivities, and comparing Cpd A with a panel of established trypanocides, were performed at the University of Glasgow.

Enzyme-Linked Immunosorbent Assay for Direct Quantification of Intracellular cAMP Concentration

Intracellular cAMP concentrations were quantified by enzyme-linked immunosorbent assay, using the Direct Cyclic AMP Enzyme Immunoassay kit (Assay Designs). Bloodstreams from trypanosomes were cultured in vitro and incubated at 37°C with or without test compounds at a density of 5×10^6 cells/mL. At predetermined time points, 2-mL samples were centrifuged at 855 *g* for 10 minutes at 4°C. The supernatant was removed, and the cell pellet was resuspended in 100 μL of 0.1 mol/L hydrochloric acid. After centrifugation at 16 000 *g* for 10 minutes, the supernatant was removed and stored at −20°C. The cAMP content was assessed by enzyme-linked immunosorbent assay, according to the manufacturer's instructions. Samples were taken in duplicate, and all assays were conducted independently ≥3 times.

Determination of In Vivo [^{3}H]-cAMP Synthesis

Ex vivo bloodstream trypanosomes were obtained from infected rats and resuspended in HMI-9 medium containing 10% fetal calf serum (FCS) medium (with 100 μmol/L inosine substituted as the purine source instead of hypoxanthine as the latter might block [^{3}H]-adenine incorporation). [^{3}H]-adenine (40 μCi) was added, and the cultures were incubated at 37°C, 5% carbon dioxide (CO_2) for 2 hours. Cells were then washed 3 times with 10 mL of HMI-9/10% FCS (+inosine, -hypoxanthine) and finally resuspended to give a cell density of 1×10^8 trypanosomes/mL. At predetermined times, 0.5-mL samples were taken and quenched by adding an equal volume of ice-cold 5% trichloroacetic acid containing 1 mmol/L adenosine triphosphate (ATP) and 1 mmol/L cAMP. Samples were centrifuged at 16 000 *g* for 2 minutes, and the supernatants stored at −20°C until [^{3}H]-cAMP extraction.

Columns loaded with 2 mL of Dowex 50WX4-400 ion-exchange resin (Sigma) were placed above 20 mL scintillation vials, and the supernatant samples were loaded onto columns. In total, 3 mL of water was added to the column to elute [^{3}H]-ATP and [^{3}H]–adenosine diphosphate. The columns were then placed above a corresponding set of alumina columns prewashed with 0.1 mol/L imidazole, and 10 mL of water was added to each Dowex column to transfer the remaining [^{3}H]-adenine nucleotides onto the alumina column. The alumina columns were then mounted above a fresh set of 20-mL scintillation vials. The [^{3}H]-cAMP was eluted from the alumina with 6 mL of 0.1 mol/L imidazole. Then 8 mL of scintillation fluid was added to each vial, and radioactivity was determined by scintillation counting. Intracellular [^{3}H]-cAMP levels were expressed as a percentage of the total pool of [^{3}H]-adenine nucleotides.

Cell Lysis Assay

This assay was performed essentially as described by Gould et al [21]. Briefly, 100 μL of HMI-9 medium containing twice the desired concentration of test compound and 18 μmol/L propidium iodide was added to a well of a 96-well plate; a well containing 100 μL of medium with propidium iodide only was set up as a control. An equal volume of medium containing bloodstream-form trypanosomes was added to each well to give a final cell density of 5×10^6/mL and propidium iodide concentration of 9 μmol/L. Fluorescence was monitored over time at 37°C and 5% CO_2 using a FLUOstar OPTIMA fluorimeter with excitation and emission filters at 544 and 620 nm, respectively.

Cell Death Assay

Bloodstream form trypanosomes were diluted in fresh HMI-9 medium to a cell density of 5×10^5 trypanosomes/mL to which the required volume of test compound, diluted in DMSO, was added to give the desired final concentration. Cultures were incubated at 37°C and 5% CO_2. Samples were taken periodically and assessed for cell density using a hemocytometer and a phase-contrast microscope at 400-fold magnification.

Cell Cycle Analysis Using Flow Cytometry

Cells were incubated with the test compounds in HMI-9 medium. After collection by centrifugation for 10 minutes at 610 *g*, cell pellets were suspended in 70% methanol–30% PBS at 4°C overnight. After storage, the cells were washed twice in PBS by centrifugation at 855 *g* for 10 minutes, finally being resuspended in PBS containing 10 μg/mL propidium iodide and ribonuclease A. The fixed cells were then incubated for 1 hour in the dark at room temperature. Finally, flow cytometry was performed using a Becton Dickinson FACSCalibur flow cytometer and using the FL2-A detector with an amplification gain of 1.75.

Nucleus/Kinetoplast Configuration Assessment Using Fluorescence Microscopy

Culture aliquots were spread onto glass slides. After drying, they were fixed overnight in methanol at −20°C. After rehydration in PBS, slides were stained with 50 μL of PBS containing 1 μg/mL 4,6-diamidino-2-phenylindole (DAPI) and 1% (wt/vol) 1,4-diazabicyclo[2.2.2]octane (DABCO) and analyzed using a Zeiss Axioskop microscope (excitation wavelength 365 nm; emission wavelength 445 nm). For each sample, >500 cells were analyzed. Cells were manually scored and assigned to the following categories: 1N1K (1 nucleus + 1 kinetoplast; G1-phase cells); 1N2K (1 nucleus + 2 kinetoplasts; early S-phase); 2N2K-early (2 nuclei + 2 kinetoplasts, no cleavage furrow; late mitosis); 2N2K-late (2 nuclei + 2 kinetoplasts, with cleavage furrow; ongoing cytokinesis); and >2N2K (aberrant cells with >2 nuclei and 2 kinetoplasts).

Mouse Infections

Young adult female NMRI mice were infected intraperitoneally with 5×10^5 bloodstream-form trypanosomes per animal. Parasitemia was monitored daily in tail blood and reached $>10^8$/mL at day 4 in animals infected with control trypanosomes. All experiments were conducted under the rules and regulations on animal experimentation issued by the Swiss federal authorities and regularly inspected by the Committee on Animal Experimentation.

RESULTS

Two highly similar PDEs from *T. brucei*, TbrPDEB1 and TbrPDEB2, are essential for parasite survival in vitro and in vivo [11]. The extensive structural conservation between human and trypanosome PDEs [22, 23] (Hengming Ke, University of North Carolina, personal communication) allows the exploitation of current technology and expertise developed for human PDE inhibitors to be applied against parasitic diseases. Accordingly, a proprietary compound library (~400 000 compounds; Nycomed Pharma) was screened with recombinant TbrPDEB1. Hits were defined as compounds that inhibited enzyme activity by >50% at 10 μmol/L; ~600 hits were identified. All of the highly potent inhibitors belonged to 2 main chemical classes: the 4-phenyl-4a,5,8,8a-tetrahydrophthalazinones and the 4-phenyl-4a,5,6,7,8,8a-hexahydrophthalazinones (Figure 1*A*). For 35 hits, the potency to inhibit recombinant TbrPDEB1 (IC_{50}) was correlated with the potency to suppress trypanosome proliferation (half-maximal effective concentration [EC_{50}]) (Figure 1*B*). The tetrahydrophthalazinone Cpd A was identified as the most potent inhibitor of TbrPDEB1 (IC_{50}, ~10 nmol/L; Figure 1*C*), and it also inhibited the isoenzyme TbrPDEB2 with similar potency (see Figure 4*A*). For these and all subsequent experiments, Cpd A was used in a racemic form. Inhibition of TbrPDEB1 and TbrPDEB2 by Cpd A was closely paralleled by the suppression of trypanosome proliferation (Figure 1*D*). Cpd A has been disclosed as a potent inhibitor of human PDE4 (IC_{50}, 0.6 nmol/L; example 16n in reference [24]).

Cpd A inhibits cell proliferation with an EC_{50} of 30–70 nmol/L (depending on strain, inoculum density, growth medium, etc), similar to that of the trypanocides suramin or diminazene, and it is ≥10-fold more active than nifurtimox (Figure 2*A*). In addition, Cpd A is ~200-fold more potent than dipyridamole, currently the most potent inhibitor of both TbrPDEB1 and TbrPDEB2 activity [25].

Because resistance to diamidine and melaminophenyl arsenical drugs is an increasing problem [3, 4], Cpd A was

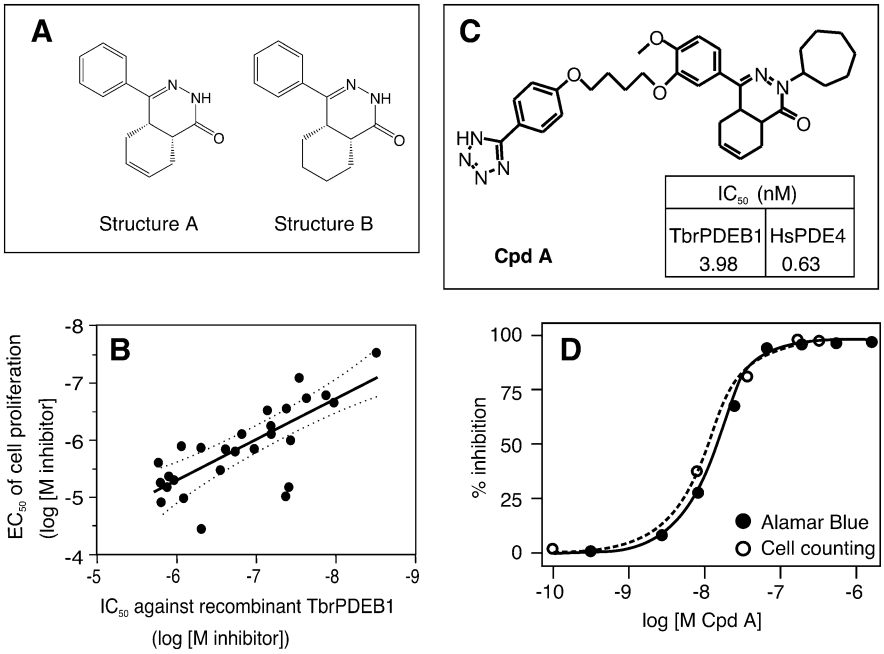

Figure 1. *A*, Structure A: 4-phenyl-4a,5,8,8a-tetrahydrophthalazinone; structure B: 4-phenyl-4a,5,6,7,8,8a-hexahydrophthalazinone. *B*, Correlation between TbrPDEB1 inhibition and trypanocidal activity by compounds of different chemical classes identified in the high-throughput screening. A best-fit line was calculated using linear regression ($r^2 = .6$), and 95% confidence intervals are indicated by dotted lines. EC_{50}, half-maximal effective concentration. *C*, Structure of compound A (Cpd A). Inset indicates half-maximal inhibitory concentration (IC_{50}) values (nmol/L) of Cpd A against TbrPDEB1 and human PDE4. *D*, In vitro trypanocidal activity of Cpd A assessed using Alamar blue (*filled circles*) or microscopic cell counts (*open circles*). After 72-hour incubation with the indicated drug concentrations. The EC_{50} values were 18 and 15 nmol/L, respectively, for the experiment shown.

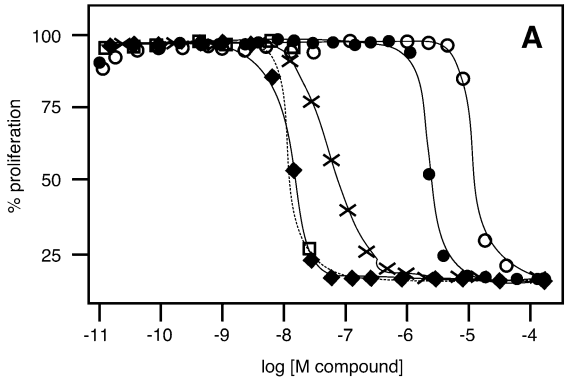

B

	EC_{50} values (nM compound)			Resistance factor	
	strains			strains	
	wt	TbAT1-KO	B48	TbAT1-KO vs wt	B48 vs wt
Compound:					
Cpd A	79 ± 10	92 ± 5	76 ± 7	1.2 *	0.96 *
Diminazene	86 ± 12	1820 ± 110	1580 ± 620	21.1 ****	18.3 **
Pentamidine	2.4 ± 0.2	7.9 ± 1.1	340 ± 59	3.3 ***	140 ***

Figure 2. *A*, Comparison of cell proliferation inhibition by compound A (Cpd A) and by other trypanocides. Diminazene aceturate (*diamonds*), suramin (*squares*), Cpd A (*crosses*), nifurtimox (*filled circles*) dipyridamole (*open circles*). Diminazene, suramin, and nifurtimox are clinically used antitrypanosomal drugs. Panel represents a single experiment that is representative of 4 identical but fully independent experiments. *B*, Trypanosome lines resistant to diminazene and pentamidine do not exhibit cross-resistance to Cpd A. B28 carries resistance to pentamidine. EC_{50}, half-maximal effective concentration; TbAT1-KO, drug-resistant derivative of MiTat1.2(221) that is resistant to diminazene [16]; wt, wild-type bloodstream forms of MiTat1.2(221). *Not significantly different from wt; $^{**}P < .05$, $^{***}P < .01$, $^{****}P < .001$.

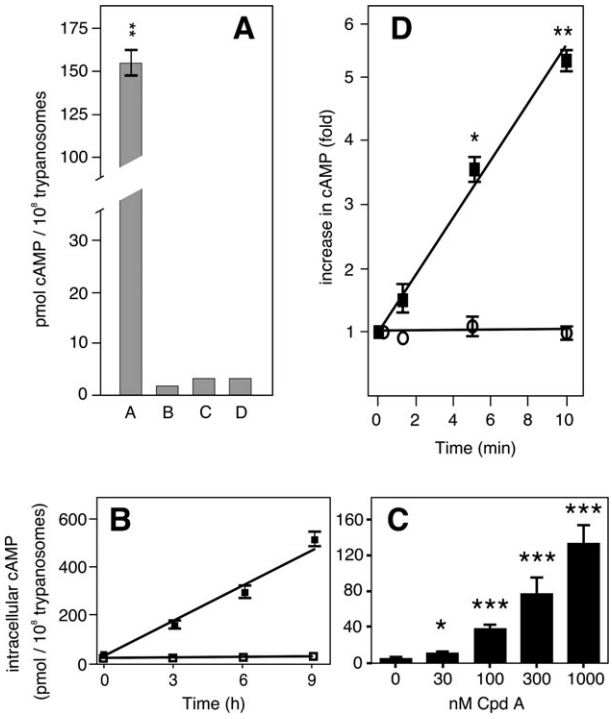

Figure 3. *A*, compound A (Cpd A) (*A*) increases intracellular cyclic adenosine monophosphate (cAMP) levels more potently than 100 μmol/L etazolate (*B*) or 40 μmol/L dipyridamole (*C*). Dimethyl sulfoxide (DMSO) control is given in *D*. Bar chart shows the intracellular cAMP concentration in bloodstream-form trypanosomes incubated with the compounds for 3 hours. Each experiment was performed in duplicate. Bars represent means (and standard error of the mean) for 3–4 independent experiments. *P* values were calculated using 2-tailed paired Student *t* test. $^{**}P < .01$. *B*, Time-dependent cAMP increase in trypanosomes incubated with 1 μmol/L Cpd A (*filled squares*) and in a control culture (DMSO only) (*open squares*). Data shown are means for 3 independent experiments; error bars indicate standard errors. *C*, Concentration dependence of cAMP accumulation. Trypanosomes were incubated with Cpd A at the indicated concentrations for 3 hours, and cAMP levels were determined by enzyme-linked immunosorbent assay. $^{*}P < .01$; $^{***}P < .001$ (2-tailed unpaired Student *t* test). *D*, Effect of 0.3 μmol/L Cpd A on intracellular cAMP levels in bloodstream-form trypanosomes (ex vivo) prelabeled for 2 hours with [^{3}H]-adenine. Cells were incubated with (*squares*) or without (*circles*) Cpd A at a cell density of 1×10^8/mL in HMI-9 medium at 37°C. Graph shown is representative of 3 separate experiments performed in triplicate. Data are expressed as fold difference relative to 0-minute control value, with standard errors.

tested for potential cross-resistance, using 2 well-defined cell lines resistant to the most important trypanocides in clinical and veterinary use today. TbAT1-KO [16] and B48 [17] are strongly resistant to diminazene (TbAT1-KO) and to all diamidine and melaminophenyl arsenical trypanocides (B48). These multidrug-resistant cell lines were as sensitive to Cpd A as were wild-type cells (Figure 2*B*).

High intracellular cAMP concentrations are lethal for bloodstream-form trypanosomes [11]. This effect can also be mimicked by membrane-permeable cAMP analogs such as 8-(4-chlorothiophenyl)-cAMP, 8-bromo-cAMP, or N6,O2'-dibutyryl-cAMP, which all inhibit cell proliferation at low micromolar concentrations. This apparent inhibition of cell proliferation by the cAMP analogs is due to progressive cell lysis, similar to what was observed when RNAi against TbrPDEB1 and TbrPDEB2 was induced [11], or after exposure of cells to Cpd A. Exposure of cultured trypanosomes to Cpd A for 3 hours raised intracellular cAMP levels 44-fold, from 3.3 ± 0.2 to 146 ± 12 pmol/10^8 cells ($P < .01$, Figure 3*A*). In contrast, the low-potency PDE inhibitors dipyridamole (40 μmol/L) and etazolate (100 μmol/L) [25] did not induce significant changes in intracellular cAMP concentrations.

The effects of Cpd A are both time and concentration dependent. At 1 μmol/L Cpd A, cAMP levels increased linearly over 9 hours (Figure 3*B*). This response is concentration dependent, and even at 30 nmol/L, Cpd A raised cAMP significantly (Figure 3*C*). The action of Cpd A occurs extremely rapidly, as determined using [^{3}H]-adenine prelabeled cells (see Materials and Methods). The concentration of cAMP

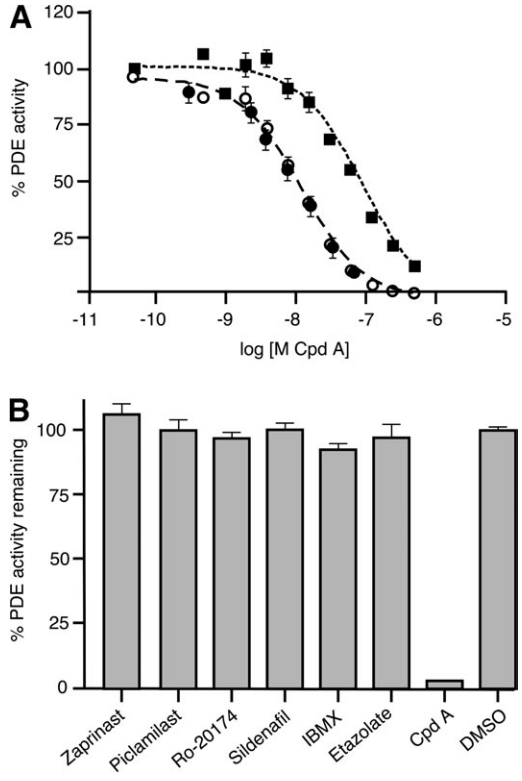

Figure 4. *A*, Potency of compound A (Cpd A) against total cellular phosphodiesterase (PDE) activity (*filled squares*) (half-maximal inhibitory concentration (IC_{50}), 76.6 nmol/L), TbrPDEB1 (*open circle*) (IC_{50}, 12.4 nmol/L) and TbrPDEB2 (*filled circles*) (IC_{50},12.0 nmol/L). All assays were performed in triplicate, and figure represents 1 of 2 independent experiments that produced essentially identical results. The slightly higher IC_{50} values (compared with Figure 1*C*; 12 vs 3.8 nmol/L) most likely reflect different enzyme sources used (Figure 1*C*, expression in SF2 cells; this figure, expression in *Saccharomyces cerevisiae*). *B*, Total cellular PDE activity inhibited at 1 μmol/L inhibitor concentration, comparing activity of Cpd A with that of reference PDE inhibitors. DMSO, dimethyl sulfoxide.

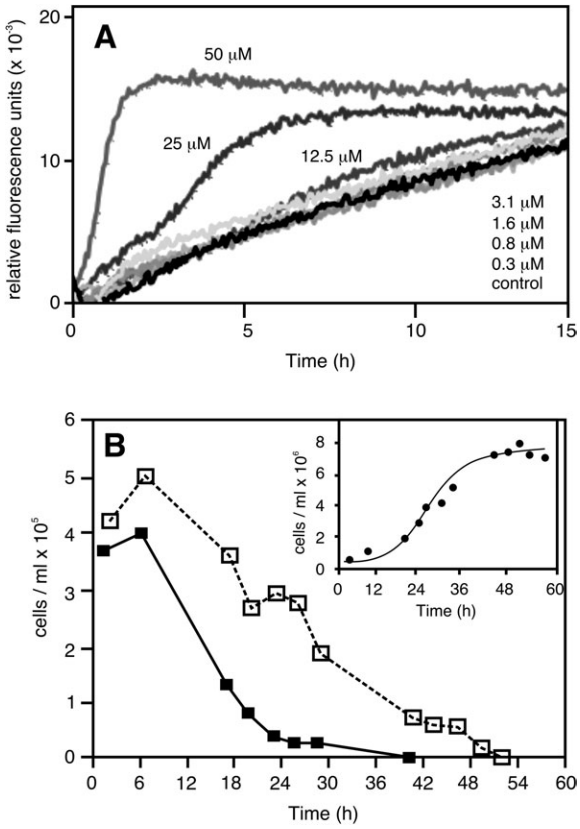

Figure 5. *A*, Cell lysis after exposure to various concentrations of compound A (Cpd A). Trypanosomes were incubated in medium containing 9 μmol/L propidium iodide (PI) and varying concentrations of Cpd A. Fluorescence was continuously monitored (excitation: 544 nm; emission 620 nm). Slow upward slope of traces corresponding to the control and low concentrations of Cpd A reflects gradual entry of PI into live, intact trypanosomes. Background fluorescence from unbound PI was subtracted. The experiment is representative of several independent experiments. *B*, Growth inhibition and cell lysis induced by Cpd A. Separate trypanosome cultures at starting densities of 4×10^5 cells/mL were incubated with 1 μmol/L (*open squares*) or 10 μmol/L (*filled squares*) Cpd A. Control culture with the same starting density was run in parallel without drug (*inset*). Cell densities were determined by microscopic counts (in duplicate) in a hemocytometer. At both concentrations tested, Cpd A induces complete cell lysis, albeit with different time courses. Panel displays a single experiment representative of several similar, independent experiments.

increased almost instantaneously after adding the compound (Figure 3*D*), demonstrating that Cpd A enters the cell rapidly and acts primarily by inhibiting PDE activity. To our knowledge, these results for the first time demonstrate the crucial role of trypanosomal PDEs in maintaining a constant low level of cAMP, counteracting a high constitutive level of cAMP synthesis [26]. Although Cpd A inhibited TbrPDEB1 and TbrPDEB2 with similar IC_{50} values of ~12 nmol/L, the IC_{50} value for inhibiting total cellular PDE activity was ~70 nmol/L (Figure 4*A*). At 1 μmol/L, Cpd A inhibited total PDE activity completely, in contrast to several reference PDE inhibitors that showed no effect at this concentration (Figure 4*B*).

Despite its rapid effect on cAMP, Cpd A had no observable effect on cell integrity for ≥15 hours, even at 3 μmol/L ($150 \times EC_{50}$) as determined by a cell lysis assay [21] (Figure 5*A*). Cell lysis is a slow process, reaching completion after 42 hours (at 10 μmol/L Cpd A) to 55 hours (at 1 μmol/L Cpd A; Figure 5*B*).

To explore cell cycle effects, trypanosomes cultured in the presence or absence of 1 μmol/L Cpd A were analyzed by flow cytometry. Control cultures displayed a constant distribution between diploid (2C) and tetraploid (4C) cells (Figure 6). In Cpd A-treated cells, the relative numbers of tetraploid cells increased progressively, whereas diploid trypanosomes diminished steadily over time. The data show that elevated cAMP levels did not immediately affect DNA synthesis but block cell cycle progression. The accumulation of higher ploidy cells (>4C) at longer incubation times suggests that

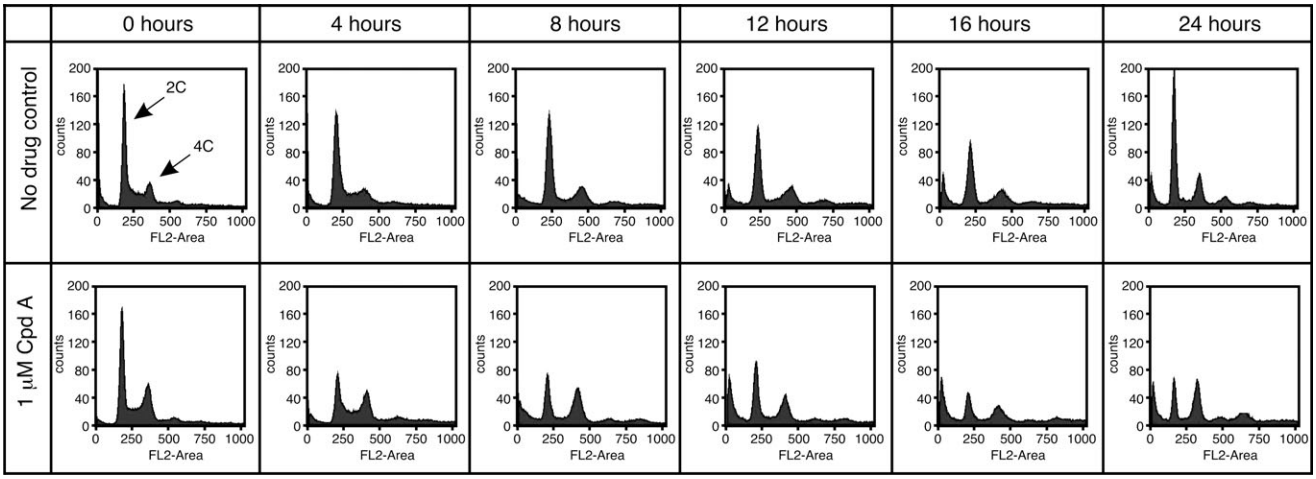

Figure 6. Flow cytometry analysis of the DNA content of trypanosomes grown in the presence and absence of 1 μmol/L compound A (Cpd A). Cells were incubated under standard culture conditions in the absence (*top row*) or presence (*bottom row*) of 1 μmol/L Cpd A. Samples were taken every 4 hours for 24 hours. Histograms indicate the number of cells with particular fluorescence intensities (that correlate with their DNA content). Peaks labeled 2C represent diploid cells; those labeled 4C represent cells that have replicated their DNA but have not yet undergone cytokinesis and thus are tetraploid. Longer incubations with Cpd A cause an increase in cells with >4C DNA content. FL2-Area: total fluorescence emission.

DNA synthesis, and possibly nuclear division, continue but without intervening cytokinesis. Fluorescence microscopy analysis of cells fixed after 12 hours of Cpd A treatment confirmed that nuclear division did take place and identified the abscission into 2 daughter cells, after near-completion of cytokinesis, as the specific defect induced by Cpd A-elevated cAMP levels. Cells were manually scored for numbers of nuclei (N) and kinetoplasts (K) and assigned to the following categories: 1N1K, 1N2K, 2N2K-early, 2N2K-late, and >2N2K (for definitions see Materials and Methods and Figure 7*A*–*F*).

For trypanosomes incubated with 1 μmol/L Cpd A, the percentage of cells in the 1N1K category (G1-phase) was reduced to 34%, compared with 74.4% in the control (Figure 7*I*). In contrast, percentages of 2N2K (late mitosis/cytokinesis) and >2N2K cells were both dramatically increased in the Cpd A-treated population. When the 3 categories corresponding to the normal cell cycle stages (1N1K, 1N2K, and 2N2K-early) were combined, this category decreased from 90.3% (controls) to 42.9% ($P < .01$) after Cpd A treatment. This was balanced by a corresponding increase in the 2N2K-late and >2N2K (aberrant cells) categories, from 9.7% (controls) to 57.1% (Cpd A treated; $P < .001$). At longer Cpd A treatments, cells become spherical, multinuclear, and multiflagellated, and they eventually lyse. This is very similar to what is seen when RNAi is induced against TbrPDEB1 and TbrPDEB2: after induction of RNAi, the cells gradually accumulate several nuclei, several kinetoplasts, and numerous flagella and finally become rounded before eventually lysing (Figure 7*G* and 7*H*).

To verify whether Cpd A-mediated cell destruction also reflects the complete elimination of trypanosome infectivity, cells were treated in vitro with 25 or 250 nmol/L Cpd A for 48 hours before infection. Groups of 5 mice were inoculated with 5×10^5 trypanosomes via intraperitoneal injection. Control trypanosomes incubated with vehicle alone caused a parasitemia of 3×10^8 cells/mL by day 4 postinfection. In contrast, trypanosomes preincubated with 250 nmol/L Cpd A were completely unable to initiate an infection. Even a preincubation with as little as 25 nmol/L Cpd A (ie, $0.5 \times EC_{50}$) dramatically reduced infectivity, with just a mild parasitemia of 5×10^6/mL reached at day 6 after infection.

We conclude that sustained high cAMP levels disrupt cell cycle regulation and inexorably lead to trypanosome death. This course of events is similar whether PDE activity is reduced with a druglike inhibitor, such as Cpd A, or by RNAi [11]. Elevated cAMP apparently has no immediate lethal effect on the cells, even at 10–100-fold excess over normal levels, but it specifically interferes with cell cycle control mechanisms, principally abscission, leading to a protracted but no less certain cell death.

DISCUSSION

This study for the first time, to our knowledge, establishes the concept of choosing as a drug target a parasite enzyme whose catalytic domain is highly conserved with human homologs that are already well explored as drug targets. Human PDEs enjoy a long story as successful drug targets, and several PDE inhibitors are on the market as medication for a wide spectrum of clinical conditions (including the human PDE3 inhibitor cilostazol (Pletal; Otsuka Pharma; for intermittent claudication), the PDE4 inhibitor roflumilast (Daxas; Nycomed Pharma; for

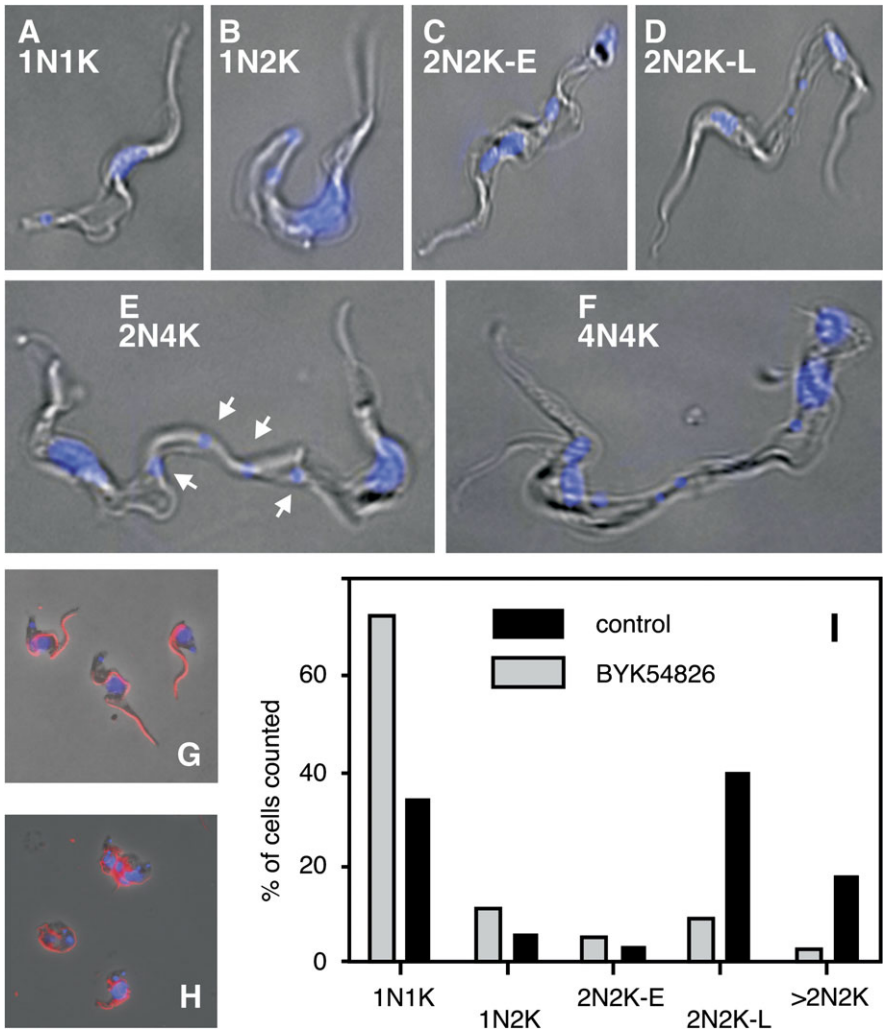

Figure 7. Images of trypanosomes incubated for 12 hours with 1 μmol/L compound A (Cpd A). Cells were stained with diamidino-2-phenylindole (DAPI) and were categorized as follows: *A*, Cell with 1 nucleus and 1 kinetoplast (1N1K). *B*, Cell with 1 nucleus and 2 kinetoplasts (1N2K). *C*, Cell with 2 nuclei and 2 kinetoplasts but before a cleavage furrow has started to divide the mother and the daughter cells (2N2K–early [E]). *D*, 2 nuclei and 2 kinetoplasts, but with cell division almost completed (2N2K–late [L]). *E*, Cell with replicated and segregated nuclei and kinetoplasts and complete cleavage furrow but not having completed mother-daughter cell separation before replicating 2 more kinetoplasts (2N4K). Arrows: kinetoplasts. *F*, Cell with 4 nuclei and 4 kinetoplasts (4N4K) with the 2 daughter cells still attached, but with each undergoing a further round of mitosis and ≥1 of the 2 daughter cells (*left side of image*) having made progress toward a further cell division. *G, H*, Normal trypanosomes before (*G*) and multiflagellated cells after (*H*) inducing RNA interference (RNAi) for TbrPDEB1 and TbrPDEB2 for 38 hours, with staining of flagellum with antibody against the paraflagellar rod (*red*) and DAPI staining of nuclei and kinetoplasts (*blue*). *I*, Percentages of cells in the various nucleus-kinetoplast configurations.

chronic obstructive pulmonary disease) or the PDE5 inhibitors sildenafil (Viagra; Pfizer), tadalafil (Cialis; Lilly ICOS) or vardenafil (Levitra; Bayer); for erectile dysfunction). Thus, a vast experience of developing PDE inhibitors from screening to registration is available and can be tapped for the development of parasite-specific PDE inhibitors. Issues concerning parasite-vs-host specificity can be addressed using the prowess of medicinal chemistry, combined with new structural information that the PDE catalytic domains show interesting parasite-specific structural features that could be exploited for rendering compounds more parasite-specific [22]. This approach of repurposing the available know-how and technology for human PDE inhibitors toward developing parasite-specific compounds may help break the deadlock between the urgent medical need for new antiparasitic drugs and the technological and financial obstacles to developing them.

Notes

Acknowledgments. The authors are grateful to Gianluca Quintini for the expression of recombinant TbrPDEB1, Xuan Lan Vu for excellent technical support, Gabriela Marti for her RNAi strains, and Yasmin Shakur and Armin Hatzelmann for continuous interest and many stimulating discussions.

Financial support. This work was supported by the Swiss National Science Foundation (grant Nr 3100A-109245 to T. S.) and the TI Pharma consortium (grant T4-302).

Potential conflicts of interest. All authors: No reported conflicts.

All authors have submitted the ICMJE Form for Disclosure of Potential Conflicts of Interest. Conflicts that the editors consider relevant to the content of the manuscript have been disclosed.

References

1. Baldauf SL. The deep roots of eukaryotes. Science **2003**; 300:1703–6.
2. Brun R, Blum J, Chappuis F, Burri C. Human African trypanosomiasis. Lancet **2010**; 375:148–59.
3. Matovu E, Seebeck T, Enyaru JCK, Kaminsky R. Drug resistance in *Trypanosoma brucei* spp., the causative agents of sleeping sickness in man and nagana in cattle. Microbes Infect **2001**; 3:763–70.
4. Seebeck T, Maeser P. Drug resistance in African trypanosomiasis. In: Mayers DL, Lerner SA, Sobel JD, Ouellette M, eds. Antimicrobial drug resistance. Vol 1. New York, NY: Humana Press, **2009**; 589–60.
5. Frearson JA, Brand S, McElroy SP, et al. N-myristoyltransferase inhibitors as new leads to treat sleeping sickness. Nature **2010**; 464: 728–32.
6. Ding D, Meng Q, Gao G, et al. Design, synthesis, and structure-activity relationship of *Trypanosoma brucei* leucyl-tRNA synthetase inhibitors as antitrypanosomal agents. J Med Chem **2011**; 54: 1276–87.
7. Jacobs RT, Nare B, Phillips MA. State of the art in African trypanosome drug discovery. Curr Top Med Chem **2011**; 11:1255–74.
8. Kunz S, Beavo JA, D'Angelo MA, et al. Cyclic nucleotide specific phosphodiesterases of the kinetoplastida: a unified nomenclature. Mol Biochem Parasitol **2006**; 145:133–5.
9. Wentzinger L, Seebeck T. Protozoal phosphodiesterases. In: Beavo JA, Francis S, Houslay M, eds. Phosphodiesterases in health and disease. Boca Raton: CRC Press, **2007**; 277–300.
10. Luginbuehl E, Ryter D, Schranz-Zumkehr J, Oberholzer M, Kunz S, Seebeck T. The N-terminus of phosphodiesterase TbrPDEB1 of *Trypanosoma brucei* contains the signal for integration into the flagellar skeleton. Eukaryot Cell **2010**; 9:1466–75.
11. Oberholzer M, Marti G, Baresic M, Kunz S, Hemphill A, Seebeck T. The *Trypanosoma brucei* cAMP phosphodiesterases TbrPDEB1 and TbrPDEB2: flagellar enzymes that are essential for parasite virulence. FASEB J **2007**; 21:720–31.
12. Cross GA. Identification, purification and properties of clone-specific antigens constituting the surface coat of *Trypanosoma brucei*. Parasitol **1975**; 71:393–417.
13. Matovu E, Geiser F, Schneider V, et al. Genetic variants of the TbAT1 adenosine transporter from African trypanosomes in relapse infections following melarsoprol therapy. Mol Biochem Parasitol **2001**; 117:73–81.
14. Matovu E, Stewart ML, Geiser F, et al. Mechanisms of arsenical and diamidine uptake and resistance in *Trypanosoma brucei*. Eukaryot Cell **2003**; 2:1003–8.
15. Bridges DJ, Gould MK, Nerima B, Mäser P, Burchmore R, de Koning HP. Loss of the high-affinity pentamidine transporter is responsible for high levels of cross-resistance between arsenical and diamidine drugs in African trypanosomes. Mol Pharmacol **2007**; 71:1098–108.
16. De Koning HP. Ever-increasing complexities of diamidine and arsenical cross-resistance in African trypanosomes. Trends Parasitol **2008**; 24:345–9.
17. Hesse F, Selzer PM, Mühlstädt K, Duszenko M. A novel cultivation technique for long-term maintenance of bloodstream form trypanosomes in vitro. Mol Biochem Parasitol **1995**; 70:157–66.
18. Lanham SM. Separation of trypanosomes from the blood of infected rats and mice by anion-exchangers. Nature **1968**; 218:1273–4.
19. Thompson WJ, Brooker G, Appleman MM. Assay of cyclic nucleotide phosphodiesterases with radioactive substrates. Methods Enyzmol **1974**; 38:205–12.
20. Bauer AC, Schwabe U. An improved assay of cyclic 3',5'-nucleotide phosphodiesterases with QAE-Sephadex columns. Nauyn Schmiedebergs Arch Pharmacol **1980**; 311:193–8.
21. Gould MK, Vu XL, Seebeck T, De Koning HP. Propidium iodide-based methods for monitoring drug action in the kinetoplastidae: comparison with the Alamar Blue assay. Anal Biochem **2008**; 382:87–93.
22. Wang H, Zier Y, Geng J, Kunz S, Seebeck T, Ke H. Crystal structure of the *Leishmania major* phosphodiesterase LmjPDEB1 and insight into the design of the parasite-selective inhibitors. Mol Microbiol **2007**; 66:1029–38.
23. Seebeck T, Sterk GJ, Ke H. Phosphodiesterase inhibitors as a new generation of anti-protozoan drugs: exploiting the benefit of enzymes that are highly conserved between host and parasite. Future Med Chem **2011**; 3:1289–1306.
24. Van der Mey M, Hatzelmann A, Van Klink GP, et al. Novel selective PDE4 inhibitors. 2. Synthesis and structure-activity relationships of 4-aryl-substituted cis-tetra- and cis-hexahydrophthalazinones. J Med Chem **2001**; 44:2523–35.
25. Zoraghi R, Kunz S, Gong KW, Seebeck T. Characterization of TbPDE2A, a novel cyclic nucleotide-specific phosphodiesterase from the protozoan parasite *Trypanosoma brucei*. J Biol Chem **2001**; 276: 11559–66.
26. Seebeck T, Gong KW, Kunz S, Schaub R, Shalaby T, Zoraghi R. cAMP signalling in *Trypanosoma brucei*. Int J Parasitol **2001**; 31:491–8.